Mott transition and magnetic collapse in iron-bearing compounds under high pressure

I. Leonov, E. Greenberg, M. P. Belov, G. Kh. Rozenberg and Igor Abrikosov

This is an electronic version of an article published in:
Leonov, I., Greenberg, E., Belov, M. P., Rozenberg, G. K., Abrikosov, I., (2017), Mott transition and magnetic collapse in iron-bearing compounds under high pressure, *High Pressure Research*, 37(2), 96-118. https://dx.doi.org/10.1080/08957959.2017.1302445

Original publication available at:
https://dx.doi.org/10.1080/08957959.2017.1302445

To appear in *High Pressure Research*
Vol. 00, No. 00, Month 20XX, 1–21

Mott transition and magnetic collapse in iron-bearing compounds under high pressure

I. Leonov[a,b,*], E. Greenberg[c,d], M. P. Belov[b], G. Kh. Rozenberg[c], and I. A. Abrikosov[e]

[a] *Theoretical Physics III, Center for Electronic Correlations and Magnetism, Institute of Physics, University of Augsburg, 86135 Augsburg, Germany*
[b] *Materials Modeling and Development Laboratory, National University of Science and Technology 'MISIS', 119049 Moscow, Russia*
[c] *School of Physics and Astronomy, Tel Aviv University, 69978, Tel Aviv, Israel*
[d] *GSEACRS, University of Chicago, Argonne, IL, USA*
[e] *Department of Physics, Chemistry and Biology (IFM), Linköping University, SE-58183 Linköping, Sweden*

(*Received 00 Month 20XX; final version received 00 Month 20XX*)

We discuss the electronic, magnetic, and related structural transitions in the iron based Mott insulators under high pressures relevant to the Earth's lower mantle conditions. The paper focuses on the above-mentioned topics based primarily on our theoretical analysis and various experimental studies employing synchrotron X-ray diffraction, ^{57}Fe Mössbauer spectroscopy, and electrical transport measurements. We review the main theoretical tools employed for the analysis of the properties of materials with strongly interacting electrons and discuss the problems of theoretical description of such systems. In particular, we discuss a state-of-the-art method for calculating the electronic structure of strongly correlated materials, the DFT+DMFT method, which merges standard band-structure techniques (DFT) with dynamical mean-field theory of correlated electrons (DMFT). We employ this method to study the pressure-induced magnetic collapse in Mott insulators, such as wüstite (FeO), magnesiowüstite ($Fe_{1-x}Mg_x$)O ($x = 0.25$ and 0.75) and goethite (FeOOH), and explore the consequences of the magnetic collapse for the electronic structure and phase stability of these materials. We show that the paramagnetic cubic $B1$-structured FeO and (Fe,Mg)O and distorted orthorhombic ($Pnma$) FeOOH exhibit upon compression a high- to low-spin (HS-LS) transition, which is accompanied by a simultaneous collapse of local moments. However, the HS-LS transition is found to have different consequences for the electronic properties of these compounds. For FeO and ($Fe_{0.75}Mg_{0.25}$)O, the transition is found to be accompanied by a Mott insulator to metal phase transition. In contrast to that, both ($Fe_{0.25}Mg_{0.75}$)O and FeOOH remain insulating up to the highest studied pressures, indicating that a Mott insulator to band insulator phase transition takes place. Our combined theoretical and experimental studies indicate a crossover between localized to itinerant moment behavior to accompany magnetic collapse of Fe ions.

Keywords: Strong correlations, high-pressure, Mott metal-insulator transition, spin-state transition, transition metal oxides

1. Introduction

During the past two decades, the strongly correlated transition metal (TM) oxides have attracted much attention because of their intriguing electronic, magnetic, and lattice

*Corresponding author. Email: Ivan.Leonov@physik.uni-augsburg.de

properties [1, 2]. These compounds often exhibit rich physics originating from the complex interplay between electronic and lattice degrees of freedom on the microscopic level. As a result, such materials often exhibit complex phase diagrams, which makes them particularly interesting in view of possible technological applications. Indeed, the great sensitivity of many correlated materials with respect to changes of external parameters such as temperature, pressure, magnetic and/or electric field, doping, etc., can be employed for the development of a new generation of elements for modern microelectronic devices and circuits.

The electronic properties of correlated oxide systems are strongly susceptible to applied pressure and/or electron/hole doping, often resulting in a Mott insulator-metal transition (IMT) caused by the mutual interplay between the Coulomb interaction between the d or f electrons and their kinetic energy [1, 2]. During the past decades, much progress has been achieved from both theoretical and experimental sides in understanding such systems. On the theory side, it has been understood that applications of state-of-the-art methods for the calculation of the electronic structure, which often provide a quantitatively correct description of the electronic, magnetic, and lattice properties of weakly correlated materials, do not lead to satisfactory results [3, 4]. These techniques cannot capture all the generic aspects of a Mott transition, such as a formation of the lower- and upper-Hubbard bands, coherent quasiparticle behavior and strong renormalization of the electron masses in the metallic phases near the Mott insulator-metal transition (IMT), etc., because of the neglect of the effect of strong correlations of localized d or f electrons [1, 2]. Therefore applications of standard band-structure methods cannot provide a quantitative description of the electronic and lattice properties of correlated materials. In particular, at ambient pressure, such techniques notoriously predict a metallic behavior for many Mott insulators, e.g., FeO and CoO, which are, in fact, wide-gap Mott insulators.

In the past decades, a significant progress in theoretical understanding of strongly correlated systems has been achieved due in part to development of dynamical mean-field theory (DMFT) of strongly correlated electrons [5, 6]. Its combination with standard band-structure methods allows one to compute the electronic, magnetic, and structural properties of correlated electron materials [7, 8]. The DFT+DMFT approach combines the ability of density functional theory (DFT) to compute the electronic structure from first principles with the systematic non-perturbative treatment of the electron correlation effects provided by using the DMFT. It allows one for a detailed quantum mechanical description of the electronic structure of strongly correlated materials. Indeed, in contrast to standard band-structure methods, which fail to describe the correct electronic properties of correlated materials, the DFT+DMFT technique allows one to treat the electron correlation effects of localized d or f electrons exactly, by neglecting only the effect of non-local correlations in a standard, single-impurity implementation of the DFT+DMFT. Hence, using this advanced theory it becomes possible to determine the electronic structure of paramagnetic correlated materials at finite temperatures, e.g., near a Mott insulator-metal transition [1, 2]. Moreover, the DFT+DMFT approach is able to determine correlation-induced structural transformations in both paramagnetic solids and long-range ordered solids, i.e., it overcomes the limitations of conventional band-structure methods and opens the way for fully microscopic investigations of the structural properties of strongly correlated systems.

So far, applications of DFT+DMFT have been successfully used for the interpretation and prediction of, e.g., photoemission, x-ray absorption, Mössbauer spectroscopy, angle-resolved photoemission experiments, etc. For instance, the DFT+DMFT method has been widely employed in recent studies of the electronic and magnetic properties of d and f transition metals and their oxides, superconducting materials, etc [9–31]. Very

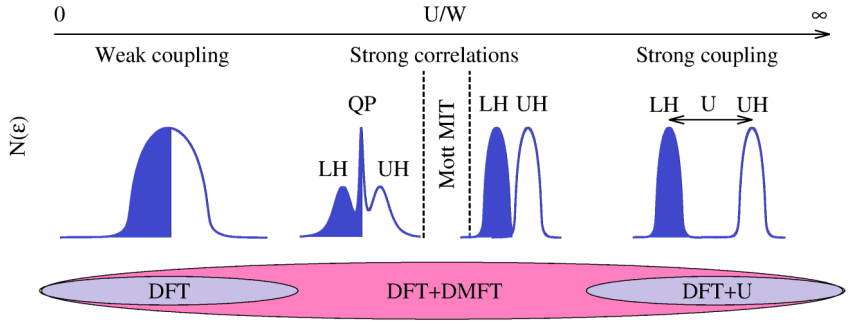

Figure 1. A schematic picture showing the ability of the present theoretical methods to determine the properties of strongly correlated materials w.r.t their correlation strength (relation between the Coulomb interaction U and the bandwidth W). LS/UH is the lower/upper Hubbard band. QP: quasiparticle peak.

recently the DFT+DMFT computational scheme has been shown to be able to treat both the electronic properties and the structural stability of strongly correlated materials on the same footing, employing a novel implementation of DFT+DMFT in combination with plane-wave pseudopotentials [13, 32–34]. It becomes possible to determine atomic displacements and hence structural transformations caused by electronic correlations using the total-energy calculations [32–37]. This method allows us to compute the evolution of the electronic properties, magnetic state, and structural transformations near the pressure-induced Mott IMT in TM oxides [13, 14], a problem posing a great theoretical and experimental challenge.

In the present work, we demonstrate a few examples of the successful use of such a theoretical approach in the case of the Fe-based Mott insulators. We discuss a number of archetype ferrous and ferric Mott insulating compounds, namely, wüstite (FeO), magnesiowüstite ($Fe_{1-x}Mg_x$)O ($x = 0.25$ and 0.75), and iron oxyhydroxide (FeOOH) at pressure conditions relevant to the Earth's lower mantle. We review a recent progress in theoretical description of strongly correlated materials, such as Mott insulators, and the ability of DFT+DMFT to describe the electronic structure, magnetic state, and phase stability of such systems near a Mott transition. The paper is organized as follows. In Section 2 we review the DFT+DMFT computational method. We present a detailed formulation of the fully charge self-consistent DFT+DMFT scheme implemented with plane-wave pseudopotentials. This method allows us to compute structural transformations, e.g., structural phase stability, caused by electronic correlations. Furthermore, we present a series of applications of the DFT+DMFT to compute the properties of wüstite ($Fe^{2+}O$), magnesiowüstite ($Fe^{2+}_{1-x}Mg_x$)O ($x = 0.25$ and 0.75), and iron oxyhydroxide ($Fe^{3+}OOH$). These applications are summarized in Section 3. In particular, we discuss the pressure-induced changes in the electronic and magnetic state, and explore the consequences of the magnetic collapse for the electronic structure and phase stability of these materials. Finally, the results of our paper are summarized in Section 4.

2. DFT+DMFT method

We start by presenting a formulation of the DFT+DMFT method which provides a robust computational tool to study the properties of strongly correlated electron systems [7, 8]. Employing this approach, it becomes possible to determine the electronic properties and structural transformations caused by electronic correlations of strongly correlated materials in their paramagnetic and long-range magnetically ordered state.

The DFT+DMFT method provides a systematic many-body treatment of the effect of strong electron correlations. This allows us to compute the properties of systems with

arbitrary correlation strength and electron filling. Thereby, the DFT+DMFT method makes it possible to interpolate two previously distinct limits (as schematically shown in Fig. 1): the limit of weakly correlated materials, which properties are often well described by DFT, and the limit of strong (nearly static) correlations as in the case of the long-range magnetically ordered wide-gap Mott insulators. For the latter case, the static mean-field techniques, such as the so-called DFT+U [3, 38], can often give reliable results. Most importantly, using the DFT+DMFT techniques it becomes possible to investigate the Mott insulator-metal transition, as well as the electronic and structural properties of materials near the Mott transition. Furthermore, with DFT+DMFT it becomes possible to treat quantum paramagnets since the method includes all local spin/charge fluctuation effects. The latter is important step forward w.r.t. the disordered local moments DFT/DFT+U techniques [39] in the realistic modeling of paramagnetic correlated materials. In fact, even in the limit of weakly correlated metals the DMFT gives more reliable description of the electronic structure, in comparison to standard DFT calculations, as has been demonstrated for the hcp Fe [40] and Os [41].

As a starting point, in this work we compute the band structure of a material of interest by using, e.g., a plane-wave pseudopotential technique [42, 43]. The results of DFT calculations, namely, the electron wave-functions and dispersion relations are further employed to construct a basis set of atomic-centered symmetry-constrained Wannier functions [44–47]. This method allows us to build up an effective low-energy Hamiltonian $\hat{H}_{DFT}$ for the correlated orbitals of interest, e.g., d or f orbitals of transition-metal ions. The Hamiltonian $\hat{H}_{DFT}$, which provides a realistic description of the low-energy band structure of an investigated material, is further supplemented by the on-site Coulomb interactions for the correlated orbitals, resulting in a multi-orbital Hubbard Hamiltonian of the form (written here for simplicity within the density-density approximation)

$$\hat{H} = \hat{H}_{DFT} + \frac{1}{2} \sum_{\{m\sigma\}} U^{\sigma\sigma'}_{mm'} \hat{n}_{m\sigma} \hat{n}_{m'\sigma'} - \hat{H}_{DC}, \tag{1}$$

where $\hat{n}_{m\sigma} = \hat{c}^{\dagger}_{m\sigma} \hat{c}_{m\sigma}$ is the local density operator for the orbital m and spin σ. $U^{\sigma,\sigma'}_{m,m'}$ is the reduced interaction matrix for the spin (σ, σ') and orbital (m, m') indices. It is expressed in terms of the Slater integrals F^0,F^2, and F^4 [38, 48]. The latter in the case of $3d$ electrons are related to the local Coulomb and Hund's rule coupling as $U = F^0$, $J = (F^2 + F^4)/14$, and $F^2/F^4 = 0.625$. $\hat{H}_{DC}$ is a double-counting correction which accounts for the electronic interactions already described by DFT. The values of Coulomb repulsion U and Hunds coupling J can be evaluated using constrained DFT [49–51] and/or constrained random phase approximation (RPA) methods [52, 53] within a Wannier-functions formalism.

The many-electron Hubbard Hamiltonian (1) is then solved self-consistently by using DMFT [7, 8] with the effective impurity model treated, e.g., by the numerically exact hybridization-expansion continuous-time quantum Monte Carlo method [54]. Employing this technique, it becomes possible to describe the quantum dynamics of the many-electron problem exactly, only neglecting (in the simplest single-site approximation) by the non-local correlation effects. We note that the choice of the method for solving the effective impurity model can drastically affect final results. In particular, for the case of correlated electron materials, such as Mott insulators or strongly renormalized unconventional metals, one has to ensure that the method used provides a non-perturbative treatment of the electron correlation effects. Using perturbative approaches in this case can lead to unpredictable errors. As a result, by applying a maximum entropy method to analyze Monte Carlo data, one obtains the real-frequency spectral functions, which can be further compared to physically observable spectra.

To determine the phase stability of correlated materials, we evaluate total energy using the following expression [7, 20, 32, 33]

$$E = E_{DFT}[n(\mathbf{r})] + \langle \hat{H}_{DFT} \rangle - \sum_{m,\mathbf{k}} \epsilon_{m\mathbf{k}}^{DFT} + \langle \hat{H}_U \rangle - E_{DC}, \quad (2)$$

where $E_{DFT}[n(\mathbf{r})]$ is the DFT total energy obtained for the self-consistent charge density $n(\mathbf{r})$; the third term on the right-hand side of Eq. (2) is the sum of the DFT valence-state eigenvalues which is evaluated as the thermal average of the DFT Hamiltonian with the non-interacting DFT Greens function $G_{\mathbf{k}}^{DFT}(i\omega_n)$. $\langle \hat{H}_{DFT} \rangle$ is evaluated in the same way but using the interacting Greens function which includes corelation effects described by the self-energy. To calculate these two contributions, the summation is performed over the Matsubara frequencies $i\omega_n$, taking into account an analytically evaluated asymptotic corrections:

$$\sum_{m,k} \epsilon_{m,k}^{DFT} = T \sum_{i\omega_n,\mathbf{k}} Tr[H_{DFT}(\mathbf{k}) G_{\mathbf{k}}^{DFT}(i\omega_n)] e^{i\omega_n 0^+}. \quad (3)$$

The interaction energy $\langle \hat{H}_U \rangle$ is evaluated using the double occupancy matrix computed within a quantum Monte Carlo method. The double-counting correction E_{DC} is evaluated as the average Coulomb repulsion between the N_d correlated electrons in the Wannier orbitals $E_{DC} = UN(N-1)/2$. All the presented equations are solved self-consistently in charge density, in order to include the charge redistribute effects caused by electron correlations. Further details on particular implementations can be found in Refs. [7, 20, 32, 33, 55–58].

Using this technique, we can determine structural transformations caused by electron correlation effects, as well as to evaluate the corresponding change in the atomic positions and of the unit-cell shape. The obtained result can be further employed to explain the experimentally observed structural data and to predict structural properties of real correlated materials. We apply this advanced theory to compute the electronic structure, magnetic state, and phase stability of a series of Fe bearing Mott insulating oxides at extreme conditions.

3. Magnetic collapse and Mott transition in Mott insulators under extreme conditions

The theoretical studies of the pressure-induced Mott insulator-metal transition is one of the most challenging areas of current research in solid state physics. In this chapter, we discuss the electronic, magnetic, and structural transitions in Mott insulators under high pressures relevant to the Earth's lower mantle conditions. As an example, we consider the archetype Fe-based Mott insulators, such as wüstite (FeO) [34, 36], magnesiowüstite $(Fe_{1-x}Mg_x)O$ ($x = 0.25$, 0.75), and iron oxyhydroxide (FeOOH) [59]. The main focus is given to the pressure-induced changes in their electronic structure and magnetic state, in order to explore the consequences of the magnetic collapse for the electronic structure and phase stability of these materials.

We show that the paramagnetic cubic $B1$-structured FeO and (Fe,Mg)O and distorted orthorhombic ($Pnma$) FeOOH exhibit (upon compression) a high- to low-spin (HS-LS) transition, which is accompanied by a simultaneous collapse of local moments. However, the HS-LS transition is found to have different consequences for the electronic properties of these compounds. For FeO and $(Fe_{0.75}Mg_{0.25})O$, the transition is associated with a

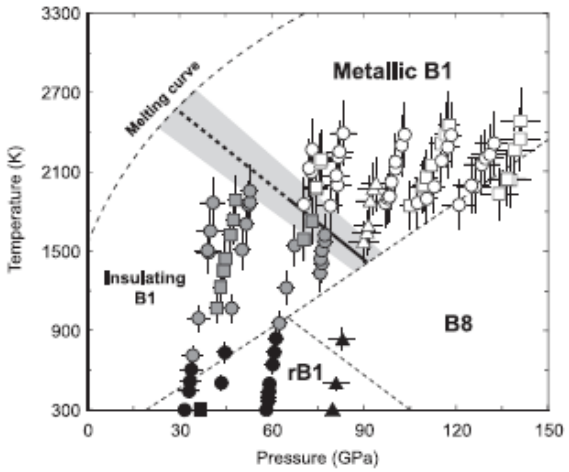

Figure 2. Phase diagram of FeO [69]. Stability of $rB1$, insulating $B1$, and metallic $B1$ phases are represented by solid, gray solid and open symbols, respectively. Circles, squares and triangles indicate each set of experiments. A metal-insulator transition boundary shown as bold line is determined from present data, and linearly extrapolated to the melting condition (broken bold line). The estimated uncertainty in location of the transition is shown by gray band.

Mott IMT. In contrast to that, both $(Fe_{0.25}Mg_{0.75})O$ and FeOOH remain insulating up to the highest studied pressures, indicating that a Mott insulator to band insulator phase transition takes place. Our results also indicate a crossover between localized to itinerant moment behavior to accompany magnetic collapse of Fe ions.

3.1. *FeO*

The high-pressure behavior of wüstite, FeO, has attracted much recent attention from both experimental and theoretical point of views [60–63]. It is one the basic oxide components of the Earth's interior. Therefore the electronic properties and phase stability of FeO is of fundamental importance for understanding the properties and evolution of the Earth's lower mantle. FeO has a relatively complex pressure-temperature phase diagram (see Fig. 2) [64–68] originating from complex interplay between the effect of electron correlations and lattice [34, 69, 70]. Under ambient conditions, it is a paramagnetic Mott insulator with a rock-salt cubic $B1$ crystal structure. It is antiferromagnetic below the Neel temperature $T_N \sim 198$ K. The Neel transition is accompanied by a structural transition from the $B1$ to the rhombohedral $R\bar{3}c$ phase ($rB1$).

Shock-wave compression and electrical conductivity measurements showed a possible appearance of a high-pressure metallic phase of FeO above ~ 70 GPa [71]. On the basis of high-pressure Mössbauer spectroscopy measurements [63, 72–74], the transition to a metallic state was assigned to a high- to low-spin transition (HS-LS), which has been proposed by band-structure calculations to occur above $\sim$ 100-200 GPa [75]. On the other hand, x-ray emission spectroscopy reveals the HS state of Fe up to ~ 140 GPa (at room temperature), while it is found to transform to the LS state upon further heating [76, 77]. On the basis of these measurements, the insulator-to-metal HS-LS transition has long been considered to be due to a structural transformation from the $B1$ to $B8$ structure. In contrast to that, recent experiments have shown that the $B1$-type FeO undergoes a high-temperature insulator-to-metal transition at about 70 GPa, retaining the same $B1$ lattice structure [69]. Moreover, the $B1$-type structure has been shown to remain stable at high pressure and temperature, being the stable phase along the geotherm through the Earth's mantle and outer core [69].

To explore the high-pressure behavior of FeO, we compute its electronic structure, mag-

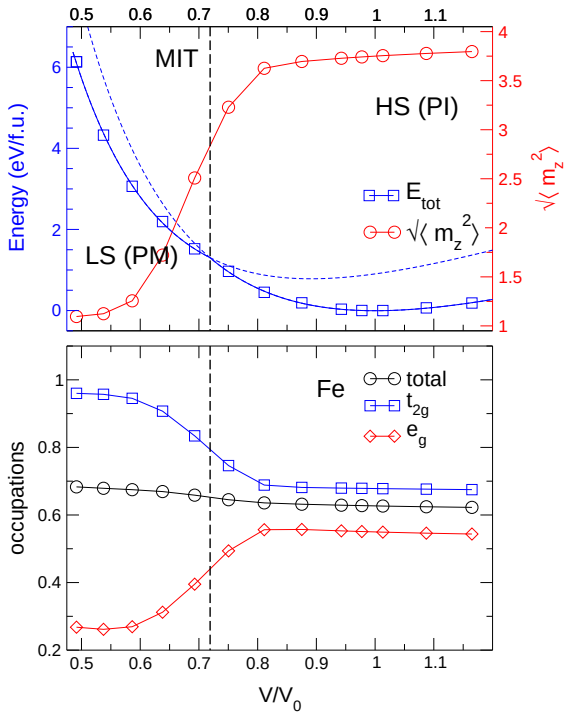

Figure 3. DFT+DMFT total energy (blue line) and local moment $\sqrt{\langle m_z^2 \rangle}$ (red line) of paramagnetic B1-type FeO calculated by DFT+DMFT for different volumes (top). PI: HS paramagnetic insulating phase. PM: LS metal. The calculated equation of state is depicted by solid blue line. The metastable solutions are shown by dotted blue lines. The HS-LS state transition is depicted by a vertical black dashed line. Bottom: Fe $3d$ and partial t_{2g} and e_g occupations as a function of volume.

netic state, and phase stability employing the fully charge self-consistent DFT+DMFT method [34, 69]. In these calculations, we neglect the structural complexity of FeO under pressure [64–69] and study the properties of the B1-structured phase of FeO which was shown to be the stable phase along the geotherm through the Earth's lower mantle. Below we denote the compressed phase by the relative volume w.r.t. the calculated equilibrium lattice volume as $\sim$ V/V$_0$. The details of these calculations are summarized in Refs. [34, 36]. The calculations are performed for the paramagnetic state at an electronic temperature T=1160 K, relevant for the Earth's lower mantle conditions. We use the average Coulomb interaction $U = 7$ eV and Hund's exchange $J = 0.89$ eV for the Fe $3d$ shell, in accordance with previous estimates [4, 36, 69]. These values are assumed to remain constant (for simplicity) upon variation of the lattice volume.

Our results for the evolution of the total energy and (instantaneous) local magnetic moments of paramagnetic FeO as a function of lattice volume are presented in Fig. 3 (top). Using these results, we evaluate equation of states by fitting the calculated total energy to the third-order Birch-Murnaghan equations of state separately for the HS and LS regions. Our results are in overall good agreement with available experimental data [67–69]. In particular, at ambient pressure we obtain a Mott insulator with a large d-d energy gap of $\sim$ 2 eV, in accordance with optical and photoemission experiments [78]. The energy gap of about 0.8 eV lies between the top of the valence band originating from the mixed Fe $3d$ and O $2p$ states and the empty Fe $4s$ states (in the Γ-point of the Brillouin zone as seen from our **k**-resolved spectral function calculations [34]). Our result for the equilibrium lattice constant a = 8.36 a.u. is less than 1-2 % off the experimental value (shown in Table 1). The calculated bulk modulus $B = 140$ GPa and the local magnetic moment of $3.7\mu_B$, agree well with experiment. Fe t_{2g} and e_g orbital occupancies are 0.68 and 0.55, respectively. All this clearly indicates that at ambient

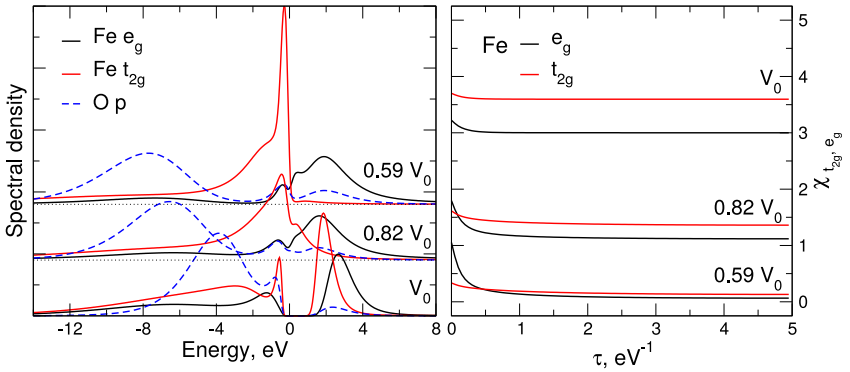

Figure 4. Left: DFT+DMFT spectral function of paramagnetic FeO for three different lattice volumes (V_0, 0.82 V_0, and 0.59 V_0). Fe t_{2g}/e_g and O p orbital contributions are shown. Right: Local magnetic susceptibility $\chi(\tau) = \langle \hat{m}_z(\tau)\hat{m}_z(0)\rangle$ calculated by DFT+DMFT for paramagnetic B1-type FeO as a function of volume. The intra-orbital t_{2g} and e_g contributions are shown. The insulator-metal transition associated with the HS-LS transformation takes place at $V/V_0 \sim 0.72$, at pressure $\sim$ 73 GPa. The calculated equilibrium volume $V_0 = 144$ a.u.^{3}.

pressure Fe^{2+} ion is in a high-spin state (S = 2). In fact, in a cubic crystal field, the Fe^{2+} ions with Fe $3d^6$ configuration, i.e., four electrons in the t_{2g} and two in the e_g orbitals, have an atomic magnetic moment of $4\mu_B$. We also point out the crucial importance of the electron correlation effects to determine the correct electronic and lattice properties of FeO. Thus, in contrast to the experiment, standard band-structure methods give a metallic solution for FeO.

Our results indicate that upon compression FeO undergoes a high-spin (HS) to low-spin (LS) transition [63], with a collapse of the local moment to a LS state, with local magnetic moment (evaluated as $M_z = \sqrt{T\int_0^{1/T} d\tau \langle m_z(\tau)m_z(0)\rangle}$, where T is the temperature) below $\sim 0.7\ \mu_B$ at pressure above 160 GPa, i.e., $V/V_0 < 0.6$. Upon the transition, we observe a substantial redistribution of charge between the Fe t_{2g} and e_g orbitals within the Fe $3d$ shell [shown in Fig. 3 (bottom)]. It results in a (almost) completely occupied state with the t_{2g} occupation of about 0.95 at high pressures, whereas the e_g orbitals are strongly depopulated (their occupation is only 0.25). The spin-state transition is found to be accompanied by a collapse of lattice volume. The structural change takes place upon a compression of the lattice volume to $\sim$ 0.72, i.e., at pressure 73 GPa, in good agreement with recent experimental high-temperature data [69]. It results in a collapse of the lattice volume by $\sim$ 8.5 %. In addition, we note a substantial change of the bulk modulus, which increases by $\sim$ 30 %, implying a remarkable change of the compressibility at the phase transition.

Overall, the electronic structure, the equilibrium lattice constant, and the structural phase stability of paramagnetic B1-type FeO obtained by employing the fully charge self-consistent DFT+DMFT approach are in remarkably good agreement with the recent experimental data [67–69], clearly indicating the crucial importance of electronic correlations. Moreover, the Fe $3d$ electrons are found to exhibit a crossover from a localized to itinerant magnetic behavior under pressure, implying delocalization of the $3d$ electrons at high pressures [36]. Our results reveal [34, 36] that within the $B1$ structure of FeO the HS-LS transition is accompanied by a Mott insulator-metal transition (see Fig. 4 (left)) [67, 69, 71], which results in a collapse of the lattice volume by $\sim$ 8.5 %. Moreover, our results for the local spin susceptibility $\chi(\tau)$ for different pressures [see Fig. 4 (right)] show that the HS-LS transition is accompanied a crossover from a localized to itinerant magnetic moment behavior for the Fe $3d$ electrons.

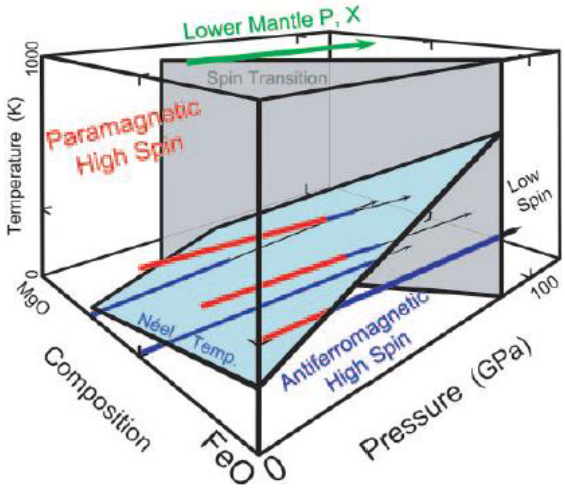

Figure 5. Summary of high-pressure ^{57}Fe Mössbauer spectroscopy results, at 6-300 K, on (Mg,Fe)O magnesiowüstite [72], which along with silicate perovskite is thought to make up the bulk of the Earth's lower mantle. At high pressures and low temperatures, magnesiowüstite is antiferromagnetic (blue lines), with a site magnetization that increases under pressure. A new signal indicative of a nonmagnetic (diamagnetic, black lines) site appears abruptly at pressures above 30-90 GPa, depending on composition, and is interpreted as the onset of the high- to low-spin transition (gray surface). For mantle compositions, with bulk Mg/(Mg+Fe) ratio as high as $x = 0.9$, the spin transition occurs at pressures as low as 30-40 GPa, corresponding to the shallowest part of the lower mantle. This figure illustrates only a subset of pressure-temperature paths explored for various compositions, with spectra also being collected as a function of temperature at constant pressure (see also Ref. [63]).

3.2. *$(Fe_{1-x}Mg_x)O$ magnesiowüstite with $x = 0.25$ and 0.75*

To proceed further, we discuss the electronic structure, magnetic state, and lattice properties of the B1-structured $(Fe_{1-x}Mg_x)O$, with $x = 0.25$ and 0.75. This material is known to exist at ambient conditions as a solid solution between MgO periclase and FeO wüstite. It is the second most abundant mineral in the Earth's lower mantle. Because of this understanding the high-pressure properties of (Fe,Mg)O is important for modeling of mineralogical composition of the Earth's lower mantle, as well as for interpreting of the (indirect) geophysical observations, e.g., in seismology [61, 67, 72, 77, 79, 80].

Our results presented in the previous chapter show that the paramagnetic $B1$-type structured FeO undergoes a corroborating HS-LS and Mott IMT at $\sim$ 73 GPa which is accompanied by a a substantial drop of the volume by $\sim$ 8.5 %. One can expect that similar behavior associated with the magnetic collapse of Fe ions occurs in (Fe,Mg)O under pressure. Indeed, recent experimental studies (which are summarized in Fig. 5) indicate that the HS-LS transition in (Fe,Mg)O occurs at a pressure range relevant for the Earth's lower mantle [72, 74]. While there is a substantial scattering in the results for the spin-state transition pressure, it was found that the transition pressure decreases upon increase of Mg content. This can be understood that due to the smaller size of Mg, Mg content acts as an effective chemical pressure on the HS Fe^{2+}. In addition, x-ray diffraction studies show that addition of Mg tends to stabilize the rock-salt $B1$ structure to high pressures and temperatures, indicating that magnesiowstite is presumably stable in the $B1$-type structure in the Earth's lower mantle.

We now explore the high-pressure behavior of B1-type $(Fe_{1-x}Mg_x)O$ for two particular compositions $x = 0.25$ and 0.75, and compute the electronic state and phase stability using the fully charge self-consistent DFT+DMFT method. These calculations are performed in the paramagnetic state at an electronic temperature T=1160 K, relevant for the Earth's lower mantle conditions. To model the chemical disorder, we employ supercell calculations containing eight formula units of the host material in which two Mg/Fe

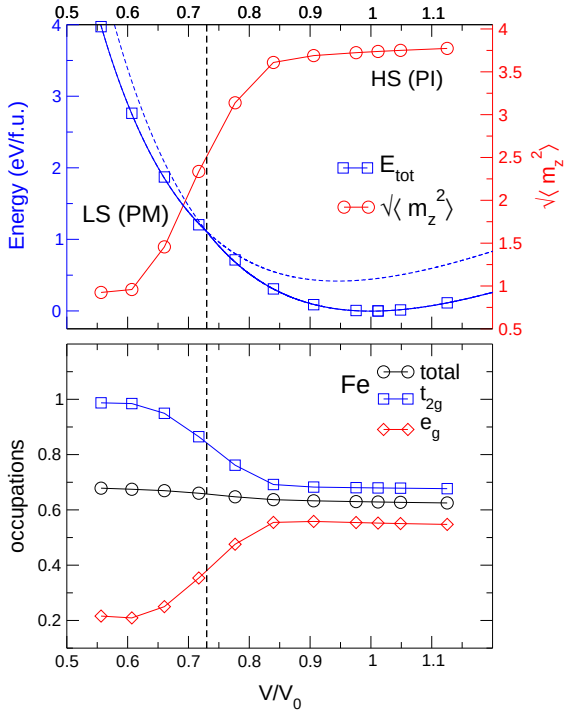

Figure 6. DFT+DMFT total energy and local moment $\sqrt{\langle m_z^2 \rangle}$ (top) and Fe $3d$ and partial t_{2g} and e_g occupations (bottom) calculated by DFT+DMFT for paramagnetic B1-type $(Fe_{0.75},Mg_{0.25})O$ as a function of lattice volume. The HS-LS state transition is depicted by a vertical black dashed line.

atoms were replaced by two Fe/Mg atoms. The positions of the impurity atoms were chosen to maximize a distance from each other (Fe/Mg atoms are uniformly distributed over the unit cell, i.e, we neglect possible formation of the Fe/Mg clusters under pressure [73]). For simplicity, we neglect the local relaxation effects around the impurity Mg/Fe atoms. In accord with the previous studies of FeO, we use the same average Coulomb interaction $U = 7$ eV and Hund's exchange $J = 0.89$ eV for the Fe $3d$ shell, which (for simplicity) are fixed upon variation of the lattice volume.

In Figs. 6 and 7 we display the evolution of the total energy and (instantaneous) local magnetic moments of paramagnetic B1-structured (Fe,Mg)O for different volumes. The corresponding equation of states are constructed by fitting the calculated total energy to the third-order Birch-Murnaghan equation of states separately for the HS and LS volume regions. Our findings are in overall good agreement with available experimental data [72, 74, 77, 79, 81]. In particular, at ambient pressure we obtain a Mott insulating solution for both $x = 0.25$ and 0.75 with a large d-d energy gap of ~ 2 eV, in accordance with transport measurements [70]. Our results for the equilibrium lattice constant, bulk modulus, and (instantaneous) local magnetic moment agree well with experiments and are summarized in Table 1. For both compositions of (Fe,Mg)O, at ambient pressure, the Fe t_{2g} and e_g orbital occupancies are large 0.68 and 0.55, respectively, implying the HS (S = 2) state of Fe^{2+} ions. Indeed, the calculated (instantaneous) magnetic moment is about 3.7 μ_B (corresponding to the fluctuating (local) magnetic moment of about 3.6 μ_B). We also point out the crucial importance of the electron correlation effects to determine the correct electronic and lattice properties of (Fe,Mg)O. Similarly to the case of FeO, in contrast to experimental data, band-structure techniques give a metallic solution for both discussed compositions of (Fe,Mg)O at ambient pressure.

Furthermore, our calculations show that highly pressurized (Fe,Mg)O undergoes a high-spin (HS) to low-spin (LS) transition, with a collapse of the local moment to a LS state, with fluctuating (local) magnetic moment $<$ 0.2-0.4 μ_B at pressures above 100

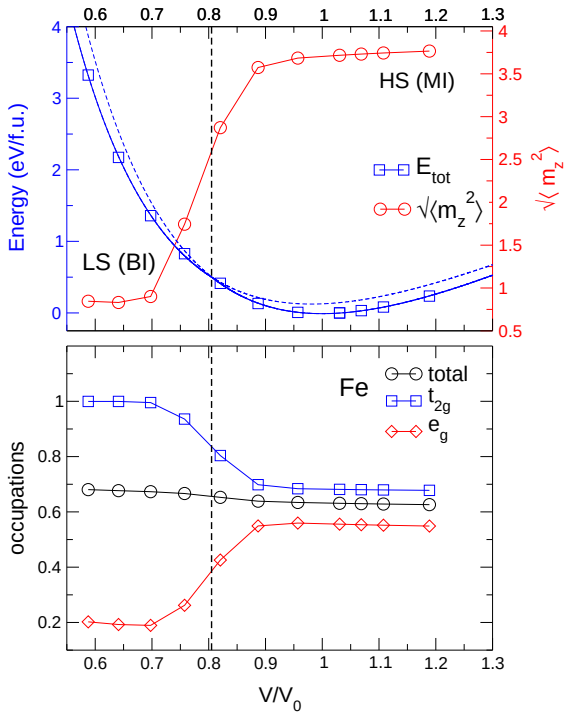

Figure 7. DFT+DMFT total energy and local moment $\sqrt{\langle m_z^2 \rangle}$ (top) and Fe $3d$ and partial t_{2g} and e_g occupations (bottom) calculated by DFT+DMFT for paramagnetic B1-structured $(Fe_{0.25},Mg_{0.75})O$ for different volumes. MI: paramagnetic Mott insulating phase. BI: LS band insulator.

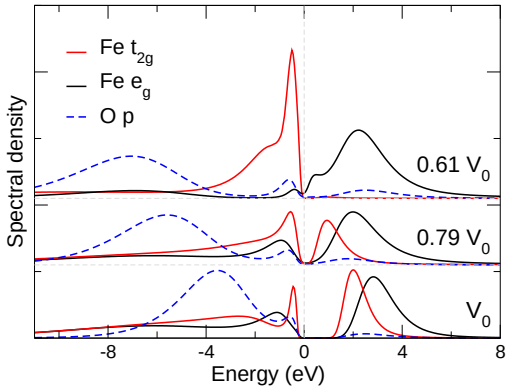

Figure 8. DFT+DMFT spectral function of paramagnetic B1-type $(Fe_{0.75},Mg_{0.25})O$ as a function of lattice volume. Fe t_{2g}/e_g and O p orbital contributions are shown. The insulator-metal transition associated with the HS-LS transformation takes place at $V/V_0 \sim 0.72$, at pressure $\sim$ 72 GPa. The calculated equilibrium volume $V_0 = 141$ a.u.^{3}.

GPa, i.e., $V/V_0 < 0.6$-0.65. Upon transition, similarly to FeO, we observe a substantial redistribution of charge between the Fe t_{2g} and e_g orbitals within the Fe $3d$ shell (shown in the bottom of Figs. 8 and 9). It results in a (almost) completely occupied t_{2g} states at high pressures, whereas the e_g orbitals are strongly depopulated (their occupation is only 0.2). The HS-LS spin-state transition is found to be accompanied by a volume drop. The structural change takes place upon a compression of the lattice volume to $V/V_0 \sim$ 0.7-0.8. The calculated transition pressures are 72 and 45 GPa for Mg content $x = 0.25$ and 0.75, respectively, in agreement with experiments. These results imply that the HS-LS transition pressure in magnesiowüstite is very sensitive to the Mg content. While for the Fe-rich magnesiowüstite, the transition pressure exhibits a rather weak variation (our

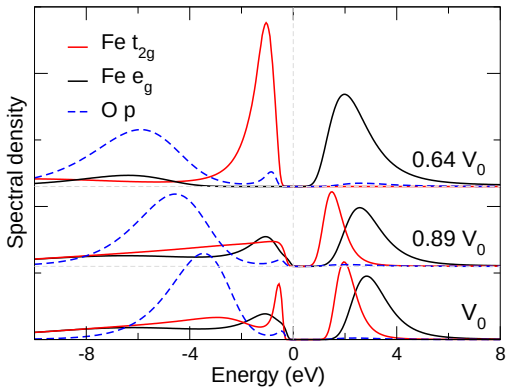

Figure 9. DFT+DMFT spectral function of paramagnetic B1-type $(Fe_{0.25},Mg_{0.75})O$ as a function of lattice volume. Fe t_{2g}/e_g and O p orbital contributions are shown. No insulator-metal transition detected at the HS-LS transformation at $V/V_0 \sim 0.8$, at pressure $\sim$ 45 GPa. The equilibrium volume $V_0 = 134$ a.u.^{3}.

results for pure FeO and 25 % of Mg essentially coincide), for the Fe-poor compounds it drops by $\sim$ 40 %. At the transition point, we obtain a substantial drop of the lattice volume by $\sim$ 5 and 3 % for the Fe-rich and poor compounds, respectively. We note however that these values should be considered as an upper-bound estimate because we neglect multiple intermediate-phase transitions when fit the total-energy result to the third order Birch-Murnaghan equation of states. Interestingly, the equilibrium bulk modulus in the Fe-poor (Fe,Mg)O (about 150 GPa) is higher than that in the Fe-rich compound (140 GPa). This also correlates with a substantial decrease of the equilibrium lattice volume of (Fe,Mg)O by $\sim$ 6-7 % upon addition of Mg.

Overall, the electronic structure, the equilibrium lattice constant, and the structural phase stability of paramagnetic (Fe,Mg)O obtained by employing the fully charge self-consistent DFT+DMFT approach are in remarkably good agreement with the experimental data, clearly indicating the crucial importance of electronic correlations. Moreover, our results indicate a substantial change in the behavior of the Fe 3d electrons, which are found to exhibit a crossover from a localized to itinerant magnetic behavior under pressure, implying delocalization of the 3d electrons at high pressures. Overall, these results are consistent with those obtained for pure FeO.

Our results for the electronic structure of paramagnetic (Fe,Mg)O reveal that the Fe-rich and poor (Fe,Mg)O, while both exhibit a HS-LS transition, behave quite differently at high pressures. In particular, for the Fe-rich (Fe,Mg)O the HS-LS transition in the $B1$ structure is found to be accompanied by a Mott insulator to metal phase transition, i.e., the paramagnetic $(Fe_{0.75}Mg_{0.25})O$ shows a (bad) metallic behavior at high pressures. In contrast to that, the Fe-poor $(Fe_{0.25}Mg_{0.75})O$ remains insulating at the HS-LS transition, even more, its energy gap tends to increase upon further compression above the HS-LS transition. Our analysis of the high-pressure behavior of self-energy of the Fe-poor $(Fe_{0.25}Mg_{0.75})O$ compound indicates that magnetic collapse is accompanied by a Mott insulator to band insulator phase transition. In both compounds, the HS-LS transition results in a substantial drop of the lattice volume by $\sim$ 3-5 %. Moreover, the magnetic properties of (Fe,Mg)O under high-pressures are characterized by a localized to itinerant magnetic moment behavior transition of the Fe 3d electrons.

We note that our results qualitatively agree well with those proposed by J. Kunes and V. Krapek [82] for the generic phase diagram of a HS-LS transition in a two-orbital Hubbard model. In particular, addition of Mg can be understood as an effective chemical pressure on the HS Fe^{2+}, which renormalizes the effective Coulomb interaction strength to bandwidth ratio. This effect leads to a direct HS Mott insulator to LS band insulator phase transition (without an intermediate metallic state) upon increase of the crystal field

	V_0 (a.u.^{3})	K_0 (GPa)	$P_{\rm tr.}$ (GPa)	$\Delta V/V$ (%)
FeO	144	142	72.8	9
$(Fe_{0.75}Mg_{0.25})O$	141	137	72.5	5
$(Fe_{0.25}Mg_{0.75})O$	134	151	45.5	3

Table 1. Calculated structural parameters for the paramagnetic $B1$-structured $(Fe_{1-x}Mg_x)O$ oxides. $P_{\rm tr.}$ is calculated transition pressure; V_0 is ambient pressure volume; K_0, bulk modulus for the equilibrium phase; $K' \equiv dK/dP = 4.1$.

splitting caused by applied pressures. Our results for the paramagnetic $B1$-structured (Fe,Mg)O provide a unified picture of a HS-LS transition in these compounds. While the Fe-rich (Fe,Mg)O exhibit a rather weak variation of the electronic structure and lattice properties, the properties of the Fe-poor compounds are quite different. This appears due to a more local nature of magnetic interactions of Fe ion in the Fe-poor compounds. Indeed, the contribution of the Fe-Fe exchange interaction which tends to stabilize the HS state to much higher pressure is much weaker or even absent in the Fe-poor (Fe,Mg)O, indicating the importance of percolation effects for understanding the properties of (Fe,Mg)O.

3.3. *FeOOH*

We now turn to the mineral goethite, FeOOH, which has a distorted orthorhombic ($Pnma$) crystal structure and exists ubiquitously as rust on the Earth's surface and in its interior [83]. We note that in contrast to previously studied (Fe,Mg)O materials, in FeOOH iron has a higher oxidation state Fe^{3+}. High-pressure theoretical studies on FeOOH revealed that the Fe^{3+} ions undergo a HS-LS transition in the range of $\sim$ 8-56 GPa [84, 85]. The HS-LS transition has been shown to be concurrent with a structural transformation from the low-pressure α to the high-pressure ϵ-polymorph of FeOOH. The latter is found to occur above 5 GPa and 300 °C [86]. This remarkable discrepancy of the calculated transition pressures has led us to reinvestigate the evolution of the electronic, magnetic, and lattice properties of FeOOH under pressure.

To resolve this uncertainty, a collaborative experimental and theoretical study of the high-pressure properties of FeOOH has been performed [59]. To this end, single crystal and powder XRD, Mössbauer and Raman spectroscopy, and resistance measurements have been combined with the state-of-the-art theoretical computations of the electronic structure and phase stability of FeOOH. The Mössbauer spectroscopy results are shown in Fig. 10. On the theory side, a static mean-field variant of the DFT+DMFT method, the so-called DFT+U approach, has been employed [3, 38]. This technique provides a static mean-field treatment of the effect of strong correlations for long-range magnetically ordered solids. This simplified variant of DFT+DMFT makes it possible to investigate a subtle structural changes associated with the relative positions of H and O atoms, performing complete relaxation of the unit cell and all the atomic positions of FeOOH in the antiferromagnetic, ferromagnetic, and non-magnetic state. It becomes possible to relate the shift of positions of the non-correlated ions, such as hydrogen, with the electronic phase transitions in a correlated material.

The experimental studies reveal a gradual decrease of the lattice parameters and unit cell volume of FeOOH upon compression to $\sim$ 44 GPa (see Fig. 11). A closer examination shows a clear trend for symmetrization of the distorted FeO_6 octahedra upon compression, which is indicative of the H-bond symmetrization effects. At $\sim$ 45 GPa an isostructural phase transformation takes place, which is found to be accompanied by a collapse of lattice volume by about 11 % and vanishing of the Raman modes [59]. This behavior is associated with a transition from the HS (S=5/2) to LS (S=1/2) configura-

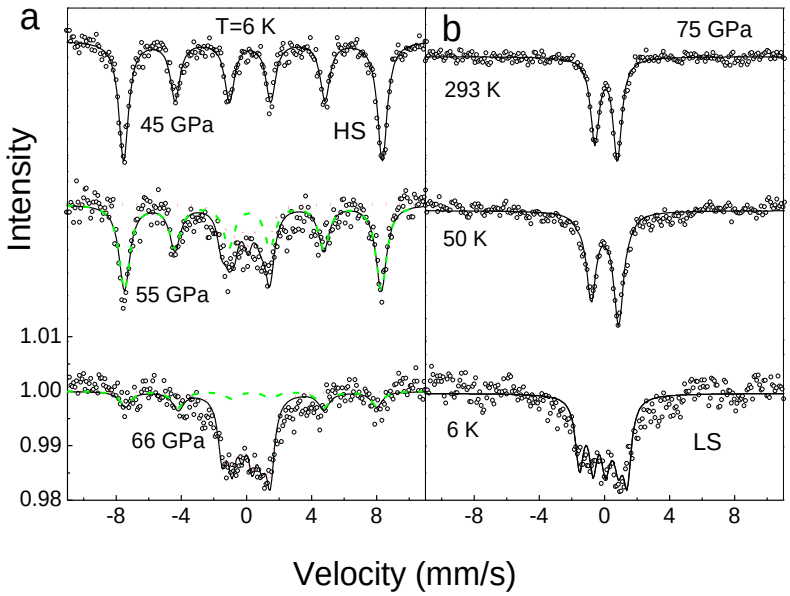

Figure 10. Mössbauer spectra of FeOOH as function of pressure at 6 K (a) and at different temperatures at 75 GPa (b) [59]. At 45 GPa the spectrum (a) can still be well fitted with a single sextet. At 55 GPa appears a new component (red dotted line), which is characterized by the significantly reduced Hhf of $\sim$ 7.2 T. This component becomes the only remaining component above 65 GPa. Upon cooling at 75 GPa a slight broadening of the doublet takes place at 50 K, followed by the onset of a magnetic splitting clearly observed at 6 K. This means a considerable drop of Neel temperature (T_N) as compared to T_N above 300 K of the low-pressure phase. Thus, the high pressure phase is characterized by the significantly reduced isomer shift and hyperfine field, lower T_N values as compared to the low pressure phase: all these changes are features of the low-spin state of Fe^{3+}.

tion in the antiferromagnetic FeOOH. Indeed, ^{57}Mössbauer spectroscopy measurements indicate the LS Fe^{3+} magnetic component appears at about 50 GPa and is characterized by smaller value of the Neel temperature. In addition to that, our resistivity data exhibit a sharp drop of 5 orders of magnitude to a non-metallic state with a significantly smaller activation energy. Therefore we conclude that the HS-LS transition in FeOOH is accompanied by an isostructural transformation, leading to a substantial drop of the lattice volume by 11 %.

The spin-state transition results in the H-bonds symmetrization, which has been confirmed by our theoretical ground-state calculations. Indeed, employing the Coulomb interaction parameter $U = 5$ eV and Hunds rule coupling $J = 1$ eV for the Fe $3d$ orbitals from the previous estimates, the DFT+U calculations [59] predict a HS-LS transition to occur at about 57 GPa in the antiferromagnetic phase of FeOOH. In Fig. 12 we display results of the total-energy calculations of antiferromagnetic FeOOH [59]. In agreement with experiment, FeOOH undergoes a HS (with magnetic moment of $4.2\mu_B$) to LS ($1.1\mu_B$) phase transition. The HS-LS transition is isostructural, resulting in a substantial drop of the lattice volume. Moreover, it is accompanied by a remarkable symmetrization of the H-bonds. Thus, the LS phase has nearly symmetric H-bonds. On the basis of resistivity measurements and band-structure calculations, we conclude that in contrast to the previously studied Fe-rich (Fe,Mg)O, FeOOH exhibits the HS-LS transition which is accompanied by a Mott to band-insulator phase transition. We argue the importance of further theoretical investigations based on the advanced DFT+DMFT approach to clarify the electronic structure and structural properties of FeOOH at high-pressures and temperatures for a better understanding of the Earth's interior. Our present studies suggest that the electronic transition of Fe in the Fe-bearing oxides at the Earth's interior conditions may affect water balance and dynamics.

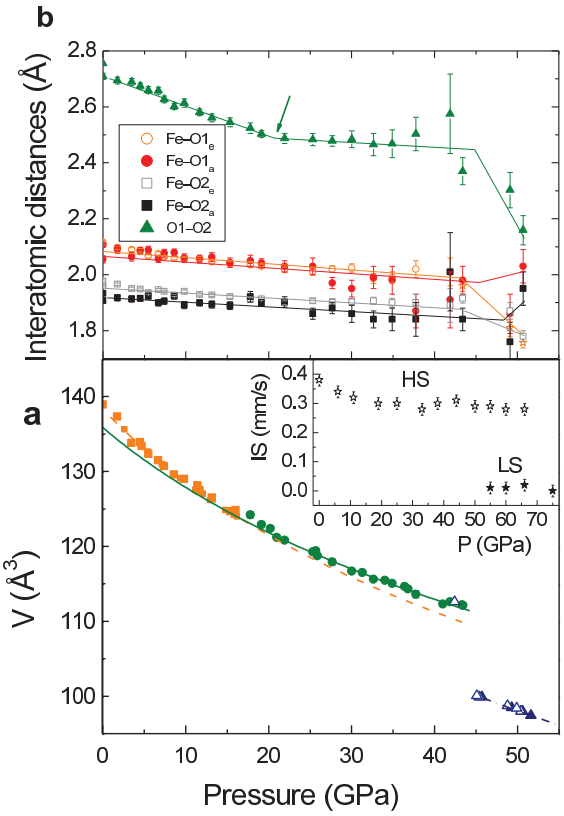

Figure 11. Pressure dependence of the lattice volume (a) and interatomic distances (b) as revealed by *in situ* x-ray diffraction measuremets [59]. Inset: pressure dependence of the isomer shift (IS) obtained from Mössbauer spectroscopy. Above $\sim$ 50 GPa an onset of the LS state is observed characterized by an abrupt drop in the IS value, signaling the sharp decrease of the average Fe-O distances.

4. Conclusions

In this paper, we review combined theoretical and experimental studies of the electronic structure, magnetic state, and structural transitions in a series of the Fe-based Mott insulating materials at extreme conditions relevant to the Earth's lower mantle conditions. We provided a detailed description of a modern theoretical technique, the DFT+DMFT approach, to calculate the electronic structure of strongly correlated materials. We employ this method to compute the pressure-induced magnetic collapse in Mott insulators wüstite (FeO), magnesiowüstite $(Fe_{1-x}Mg_x)O$ ($x = 0.25$ and 0.75) and goethite (FeOOH). In particular, we explore the consequences of the magnetic collapse for the electronic structure and phase stability of these materials in the context of their relevance for understanding the Earth's interior. Our calculations reveal that the paramagnetic cubic $B1$ structured FeO and (Fe,Mg)O and distorted orthorhombic ($Pnma$) FeOOH exhibit upon compression a HS-LS transition. The transition is accompanied by a simultaneous collapse of magnetic properties, resulting in a substantial drop of the lattice volume. However, the electronic transitions have different consequences for the spectral properties of these compounds. For FeO and $(Fe_{0.75}Mg_{0.25})O$, the transition is found to be accompanied by a Mott insulator to metal phase transition. In contrast to that, both $(Fe_{0.25}Mg_{0.75})O$ and FeOOH remain insulating up to the highest studied pressures, indicating that a Mott insulator to band insulator phase transition takes place. Our corroborative theoretical and experimental research reveals the importance of strong correlations effects to determine the properties of the Fe-bearing oxides. In particular, our results reveal a crossover between a localized to itinerant magnetic moment behavior

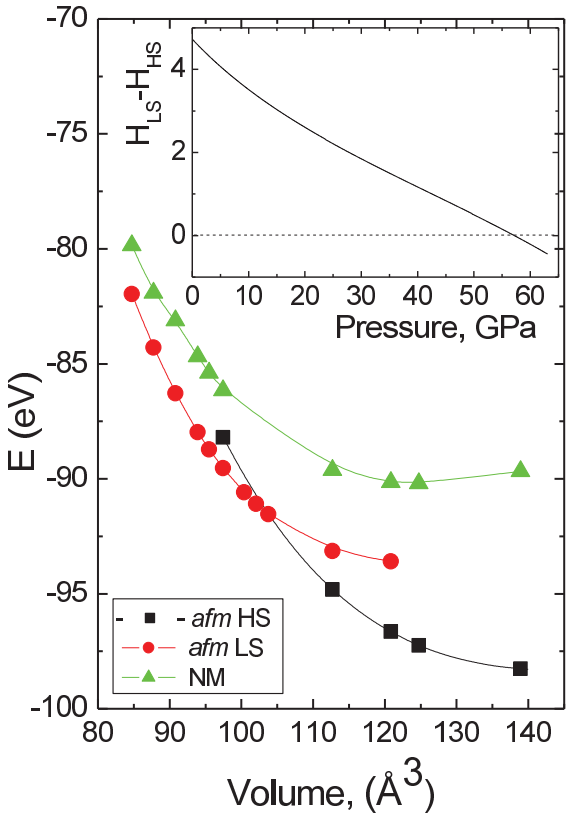

Figure 12. Dependence of the DFT+U total energies of the orthorhombic FeOOH as a function of the unit cell volume [59]. The inset shows the difference between enthalpies of the antiferromagnetic LS and HS states as a function of pressure.

which is found to accompany magnetic collapse of Fe ions. We note however that further investigations of the high-pressure properties of FeO and (Fe,Mg)O, e.g., study of their structural complexity near a HS-LS transition, are highly desirable for a better understanding of the Earth's lower mantle and outer core. We show that the DFT+DMFT approach provides a qualitative and quantitative description of the electronic properties and phase stability of all these materials, in spite of their chemical, structural, and electronic differences. The scheme is robust and makes it possible to address, on the same footing, electronic, magnetic, and structural properties of correlated materials.

5. Acknowledgements

We thank D. Vollhardt and L. Dubrovinsky for valuable discussions. I.L. acknowledges support by the Deutsche Forschungsgemeinschaft through Transregio TRR 80 and the Ministry of Education and Science of the Russian Federation in the framework of Increase Competitiveness Program of NUST "MISIS" (K3-2016-027), implemented by a governmental decree dated 16th of March 2013, N 211. M.P.B. gratefully acknowledges the financial support of the Ministry of Education and Science of the Russian Federation (Grant No. 14.Y26.31.0005) and the Russian Foundation for Basic Research (project no. 16-02-01027). I.A.A. gratefully acknowledges the Swedish Research Council (VR) grant No. 2015-04391 and the Swedish Government Strategic Research Area in Materials Science on Functional Materials at Linköping University (Faculty Grant SFO-Mat-LiU No. 2009 00971). G.K.R. and E.G. acknowledge financial support from the Israel Science Foundation under Grant no. 1489/14.

References

[1] Mott NF. Metal-insulator transition. Rev Mod Phys. 1968 Oct;40:677–683; Available from: http://link.aps.org/doi/10.1103/RevModPhys.40.677.

[2] Imada M, Fujimori A, Tokura Y. Metal-insulator transitions. Rev Mod Phys. 1998 Oct; 70:1039–1263; Available from: http://link.aps.org/doi/10.1103/RevModPhys.70.1039.

[3] Anisimov VI, Zaanen J, Andersen OK. Band theory and Mott insulators: Hubbard U instead of Stoner I. Phys Rev B. 1991 Jul;44:943–954; Available from: http://link.aps.org/doi/10.1103/PhysRevB.44.943.

[4] Mazin II, Anisimov VI. Insulating gap in FeO: Correlations and covalency. Phys Rev B. 1997 May;55:12822–12825; Available from: http://link.aps.org/doi/10.1103/PhysRevB.55.12822.

[5] Metzner W, Vollhardt D. Correlated lattice fermions in $d = \infty$ dimensions. Phys Rev Lett. 1989 Jan;62:324–327; Available from: http://link.aps.org/doi/10.1103/PhysRevLett.62.324.

[6] Kotliar G, Vollhardt D. Strongly correlated materials: Insights from Dynamical Mean-Field Theory. Phys Today. 2004;57:53–59.

[7] Georges A, Kotliar G, Krauth W, Rozenberg MJ. Dynamical mean-field theory of strongly correlated fermion systems and the limit of infinite dimensions. Rev Mod Phys. 1996 Jan; 68:13–125; Available from: http://link.aps.org/doi/10.1103/RevModPhys.68.13.

[8] Kotliar G, Savrasov SY, Haule K, Oudovenko VS, Parcollet O, Marianetti CA. Electronic structure calculations with dynamical mean-field theory. Rev Mod Phys. 2006 Aug;78:865–951; Available from: http://link.aps.org/doi/10.1103/RevModPhys.78.865.

[9] Dai X, Savrasov SY, Kotliar G, Migliori A, Ledbetter H, Abrahams E. Calculated phonon spectra of plutonium at high temperatures. Science. 2003;300:953.

[10] Savrasov SY, Kotliar G, E Abrahams E. Correlated electrons in delta-plutonium within a dynamical mean-field picture. Nature (London). 2001;410:793.

[11] Kuneš J, Korotin DM, Korotin MA, Anisimov VI, Werner P. Pressure-driven metal-insulator transition in hematite from Dynamical Mean-Field Theory. Phys Rev Lett. 2009 Apr; 102:146402; Available from: http://link.aps.org/doi/10.1103/PhysRevLett.102.146402.

[12] Grieger D, Lechermann F. Effect of chromium doping on the correlated electronic structure of V_2O_3. Phys Rev B. 2014 Sep;90:115115; Available from: http://link.aps.org/doi/10.1103/PhysRevB.90.115115.

[13] Leonov I, Anisimov VI, Vollhardt D. Metal-insulator transition and lattice instability of paramagnetic V_2O_3. Phys Rev B. 2015 May;91:195115; Available from: http://link.aps.org/doi/10.1103/PhysRevB.91.195115.

[14] Grieger D, Piefke C, Peil OE, Lechermann F. Approaching finite-temperature phase diagrams of strongly correlated materials: A case study for V_2O_3. Phys Rev B. 2012 Oct; 86:155121; Available from: http://link.aps.org/doi/10.1103/PhysRevB.86.155121.

[15] Keller G, Held K, Eyert V, Vollhardt D, Anisimov VI. Electronic structure of paramagnetic V_2O_3: Strongly correlated metallic and Mott insulating phase. Phys Rev B. 2004 Nov; 70:205116; Available from: http://link.aps.org/doi/10.1103/PhysRevB.70.205116.

[16] Amadon B, Gerossier A. Comparative analysis of models for the α-γ phase transition in cerium: A DFT+DMFT study using Wannier orbitals. Phys Rev B. 2015 Apr;91:161103; Available from: http://link.aps.org/doi/10.1103/PhysRevB.91.161103.

[17] Haule K, Birol T. Free energy from stationary implementation of the DFT+DMFT functional. Phys Rev Lett. 2015 Dec;115:256402; Available from: http://link.aps.org/doi/10.1103/PhysRevLett.115.256402.

[18] Bieder J, Amadon B. Thermodynamics of the α-γ transition in cerium from first principles. Phys Rev B. 2014 May;89:195132; Available from: http://link.aps.org/doi/10.1103/PhysRevB.89.195132.

[19] Lanatà N, Yao YX, Wang CZ, Ho KM, Schmalian J, Haule K, Kotliar G. γ-α isostructural transition in cerium. Phys Rev Lett. 2013 Nov;111:196801; Available from: http://link.aps.org/doi/10.1103/PhysRevLett.111.196801.

[20] Amadon B, Biermann S, Georges A, Aryasetiawan F. The α-γ transition of cerium is entropy driven. Phys Rev Lett. 2006 Feb;96:066402; Available from: http://link.aps.org/doi/10.1103/PhysRevLett.96.066402.

[21] McMahan AK, Held K, Scalettar RT. Thermodynamic and spectral properties of compressed Ce calculated using a combined local-density approximation and dynamical mean-field theory. Phys Rev B. 2003 Feb;67:075108; Available from: http://link.aps.org/doi/10.1103/PhysRevB.67.075108.
[22] Kuneš J, Anisimov VI, Skornyakov SL, Lukoyanov AV, Vollhardt D. NiO: Correlated band structure of a charge-transfer insulator. Phys Rev Lett. 2007 Oct;99:156404; Available from: http://link.aps.org/doi/10.1103/PhysRevLett.99.156404.
[23] Ren X, Leonov I, Keller G, Kollar M, Nekrasov I, Vollhardt D. LDA + DMFT computation of the electronic spectrum of NiO. Phys Rev B. 2006 Nov;74:195114; Available from: http://link.aps.org/doi/10.1103/PhysRevB.74.195114.
[24] Shorikov AO, Pchelkina ZV, Anisimov VI, Skornyakov SL, Korotin MA. Orbital-selective pressure-driven metal to insulator transition in FeO from dynamical mean-field theory. Phys Rev B. 2010 Nov;82:195101; Available from: http://link.aps.org/doi/10.1103/PhysRevB.82.195101.
[25] Pourovskii LV, Mravlje J, Ferrero M, Parcollet O, Abrikosov IA. Impact of electronic correlations on the equation of state and transport in ϵ-Fe. Phys Rev B. 2014 Oct;90:155120; Available from: http://link.aps.org/doi/10.1103/PhysRevB.90.155120.
[26] Belozerov AS, Leonov I, Anisimov VI. Magnetism of iron and nickel from rotationally invariant Hirsch-Fye quantum Monte Carlo calculations. Phys Rev B. 2013 Mar;87:125138; Available from: http://link.aps.org/doi/10.1103/PhysRevB.87.125138.
[27] Anisimov VI, Belozerov AS, Poteryaev AI, Leonov I. Rotationally invariant exchange interaction: The case of paramagnetic iron. Phys Rev B. 2012 Jul;86:035152; Available from: http://link.aps.org/doi/10.1103/PhysRevB.86.035152.
[28] Leonov I, Poteryaev AI, Anisimov VI, Vollhardt D. Calculated phonon spectra of paramagnetic iron at the α-γ phase transition. Phys Rev B. 2012 Jan;85:020401; Available from: http://link.aps.org/doi/10.1103/PhysRevB.85.020401.
[29] Leonov I, Poteryaev AI, Anisimov VI, Vollhardt D. Electronic correlations at the α-γ structural phase transition in paramagnetic iron. Phys Rev Lett. 2011 Mar;106:106405; Available from: http://link.aps.org/doi/10.1103/PhysRevLett.106.106405.
[30] Delange P, Ayral T, Simak SI, Ferrero M, Parcollet O, Biermann S, Pourovskii L. Large effects of subtle electronic correlations on the energetics of vacancies in α-Fe. Phys Rev B. 2016 Sep;94:100102; Available from: http://link.aps.org/doi/10.1103/PhysRevB.94.100102.
[31] Kuneš J, Lukoyanov A V, Anisimov V I, Scalettar R T, Pickett W E. Collapse of magnetic moment drives the Mott transition in MnO. Nat Mater. 2008 Mar;7(3):198; 10.1038/nmat2115; Available from: http://www.nature.com/nmat/journal/v7/n3/suppinfo/nmat2115_S1.html.
[32] Leonov I, Binggeli N, Korotin D, Anisimov VI, Stojić N, Vollhardt D. Structural relaxation due to electronic correlations in the paramagnetic insulator $KCuF_3$. Phys Rev Lett. 2008 Aug;101:096405; Available from: http://link.aps.org/doi/10.1103/PhysRevLett.101.096405.
[33] Leonov I, Korotin D, Binggeli N, Anisimov VI, Vollhardt D. Computation of correlation-induced atomic displacements and structural transformations in paramagnetic $KCuF_3$ and $LaMnO_3$. Phys Rev B. 2010 Feb;81:075109; Available from: http://link.aps.org/doi/10.1103/PhysRevB.81.075109.
[34] Leonov I. Metal-insulator transition and local-moment collapse in FeO under pressure. Phys Rev B. 2015 Aug;92:085142; Available from: http://link.aps.org/doi/10.1103/PhysRevB.92.085142.
[35] Park H, Millis AJ, Marianetti CA. Computing total energies in complex materials using charge self-consistent DFT+DMFT. Phys Rev B. 2014 Dec;90:235103; Available from: http://link.aps.org/doi/10.1103/PhysRevB.90.235103.
[36] Leonov I, Pourovskii L, Georges A, Abrikosov IA. Magnetic collapse and the behavior of transition metal oxides at high pressure. Phys Rev B. 2016 Oct;94:155135; Available from: http://link.aps.org/doi/10.1103/PhysRevB.94.155135.
[37] Leonov I, Anisimov VI, Vollhardt D. First-principles calculation of atomic forces and structural distortions in strongly correlated materials. Phys Rev Lett. 2014 Apr;112:146401; Available from: http://link.aps.org/doi/10.1103/PhysRevLett.112.146401.
[38] Liechtenstein AI, Anisimov VI, Zaanen J. Density-functional theory and strong interactions:

Orbital ordering in Mott-Hubbard insulators. Phys Rev B. 1995 Aug;52:R5467–R5470; Available from: http://link.aps.org/doi/10.1103/PhysRevB.52.R5467.

[39] Abrikosov IA, Ponomareva AV, Steneteg P, Barannikova SA, Alling B. Recent progress in simulations of the paramagnetic state of magnetic materials. Current Opinion in Solid State and Materials Science. 2016 Apr;20:85–106.

[40] Glazyrin K, Pourovskii LV, Dubrovinsky L, Narygina O, McCammon C, Hewener B, Schünemann V, Wolny J, Muffler K, Chumakov AI, Crichton W, Hanfland M, Prakapenka VB, Tasnádi F, Ekholm M, Aichhorn M, Vildosola V, Ruban AV, Katsnelson MI, Abrikosov IA. Importance of correlation effects in hcp iron revealed by a pressure-induced electronic topological transition. Phys Rev Lett. 2013 Mar;110:117206; Available from: http://link.aps.org/doi/10.1103/PhysRevLett.110.117206.

[41] Dubrovinsky L, Dubrovinskaia N, Bykova E, Bykov M, Prakapenka V, Prescher C, Glazyrin K, Liermann HP, Hanfland M, Ekholm Q M Feng, Pourovskii LV, Katsnelson MI, Wills JM, Abrikosov IA. The most incompressible metal osmium at static pressures above 750 gigapascals. Nature. 2015 Aug;525:226–229.

[42] Baroni S, de Gironcoli S, Dal Corso A, Giannozzi P. Phonons and related crystal properties from density-functional perturbation theory. Rev Mod Phys. 2001 Jul;73:515–562; Available from: http://link.aps.org/doi/10.1103/RevModPhys.73.515.

[43] Giannozzi P, Baroni S, Bonini N, Calandra M, Car R, Cavazzoni C, Ceresoli D, Chiarotti GL, Cococcioni M, Dabo I, Corso AD, de Gironcoli S, Fabris S, Fratesi G, Gebauer R, Gerstmann U, Gougoussis C, Kokalj A, Lazzeri M, Martin-Samos L, Marzari N, Mauri F, Mazzarello R, Paolini S, Pasquarello A, Paulatto L, Sbraccia C, Scandolo S, Sclauzero G, Seitsonen AP, Smogunov A, Umari P, Wentzcovitch RM. QUANTUM ESPRESSO: a modular and open-source software project for quantum simulations of materials. J Phys Condens Matter. 2009;21(39):395502; Available from: http://stacks.iop.org/0953-8984/21/i=39/a=395502.

[44] Marzari N, Mostofi AA, Yates JR, Souza I, Vanderbilt D. Maximally localized Wannier functions: Theory and applications. Rev Mod Phys. 2012 Oct;84:1419–1475; Available from: http://link.aps.org/doi/10.1103/RevModPhys.84.1419.

[45] Anisimov VI, Kondakov DE, Kozhevnikov AV, Nekrasov IA, Pchelkina ZV, Allen JW, Mo SK, Kim HD, Metcalf P, Suga S, Sekiyama A, Keller G, Leonov I, Ren X, Vollhardt D. Full orbital calculation scheme for materials with strongly correlated electrons. Phys Rev B. 2005 Mar;71:125119; Available from: http://link.aps.org/doi/10.1103/PhysRevB.71.125119.

[46] Trimarchi G, Leonov I, Binggeli N, Korotin D, Anisimov VI. LDA+DMFT implemented with the pseudopotential plane-wave approach. J Phys Condens Matter. 2008;20:135227.

[47] Korotin D, Kozhevnikov AV, Skornyakov SL, Leonov I, Binggeli N, Anisimov VI, Trimarchi G. Construction and solution of a Wannier-functions based Hamiltonian in the pseudopotential plane-wave framework for strongly correlated materials. Eur Phys J B. 2008; 65:91.

[48] Slater JC. Quantum theory of atomic structure. McGraw-Hill (New York), Volume I; 1960.

[49] Gunnarsson O, Andersen OK, Jepsen O, Zaanen J. Density-functional calculation of the parameters in the Anderson model: Application to Mn in CdTe. Phys Rev B. 1989 Jan; 39:1708–1722; Available from: http://link.aps.org/doi/10.1103/PhysRevB.39.1708.

[50] Anisimov VI, Gunnarsson O. Density-functional calculation of effective Coulomb interactions in metals. Phys Rev B. 1991 Apr;43:7570–7574; Available from: http://link.aps.org/doi/10.1103/PhysRevB.43.7570.

[51] Cococcioni M, de Gironcoli S. Linear response approach to the calculation of the effective interaction parameters in the LDA + U method. Phys Rev B. 2005 Jan;71:035105; Available from: http://link.aps.org/doi/10.1103/PhysRevB.71.035105.

[52] Aryasetiawan F, Imada M, Georges A, Kotliar G, Biermann S, Lichtenstein AI. Frequency-dependent local interactions and low-energy effective models from electronic structure calculations. Phys Rev B. 2004 Nov;70:195104; Available from: http://link.aps.org/doi/10.1103/PhysRevB.70.195104.

[53] Miyake T, Aryasetiawan F, Imada M. *Ab initio* procedure for constructing effective models of correlated materials with entangled band structure. Phys Rev B. 2009 Oct;80:155134; Available from: http://link.aps.org/doi/10.1103/PhysRevB.80.155134.

[54] Gull E, Millis AJ, Lichtenstein AI, Rubtsov AN, Troyer M, Werner P. Continuous-time

Monte Carlo methods for quantum impurity models. Rev Mod Phys. 2011 May;83:349–404; Available from: http://link.aps.org/doi/10.1103/RevModPhys.83.349.

[55] Pourovskii LV, Amadon B, Biermann S, Georges A. Self-consistency over the charge density in dynamical mean-field theory: A linear muffin-tin implementation and some physical implications. Phys Rev B. 2007 Dec;76:235101; Available from: http://link.aps.org/doi/10.1103/PhysRevB.76.235101.

[56] Aichhorn M, Pourovskii L, Vildosola V, Ferrero M, Parcollet O, Miyake T, Georges A, Biermann S. Dynamical mean-field theory within an augmented plane-wave framework: Assessing electronic correlations in the iron pnictide LaFeAsO. Phys Rev B. 2009 Aug;80:085101; Available from: http://link.aps.org/doi/10.1103/PhysRevB.80.085101.

[57] Amadon B, Lechermann F, Georges A, Jollet F, Wehling TO, Lichtenstein AI. Plane-wave based electronic structure calculations for correlated materials using dynamical mean-field theory and projected local orbitals. Phys Rev B. 2008 May;77:205112; Available from: http://link.aps.org/doi/10.1103/PhysRevB.77.205112.

[58] Haule K. Quantum Monte Carlo impurity solver for cluster dynamical mean-field theory and electronic structure calculations with adjustable cluster base. Phys Rev B. 2007 Apr; 75:155113; Available from: http://link.aps.org/doi/10.1103/PhysRevB.75.155113.

[59] Xu W, Greenberg E, Rozenberg GK, Pasternak MP, Bykova E, Boffa-Ballaran T, Dubrovinsky L, Prakapenka V, Hanfland M, Vekilova OY, Simak SI, Abrikosov IA. Pressure-induced hydrogen bond symmetrization in iron oxyhydroxide. Phys Rev Lett. 2013 Oct;111:175501; Available from: http://link.aps.org/doi/10.1103/PhysRevLett.111.175501.

[60] F GA, Struzhkin VV, Jacobsen SD. Reduced radiative conductivity of low-spin (Mg,Fe)O in the lower mantle. Science. 2006;312:1205.

[61] Lin JF, Vank G, Jacobsen SD, Iota V, Struzhkin VV, Prakapenka VB, Kuznetsov A, Yoo CS. Spin transition zone in Earth's lower mantle. Science. 2007;317:1740.

[62] Ozawa H, Takahashi F, Hirose K, Ohishi Y, Hirao N. Phase transition of FeO and stratification in Earth's outer core. Science. 2011;334:792.

[63] Pasternak MP, Taylor RD, Jeanloz R, Li X, Nguyen JH, McCammon CA. High pressure collapse of magnetism in $Fe_{0.94}O$: Mössbauer spectroscopy beyond 100 GPa. Phys Rev Lett. 1997 Dec;79:5046–5049; Available from: http://link.aps.org/doi/10.1103/PhysRevLett.79.5046.

[64] Fei Y, Mao HK. In situ determination of the NiAs phase of FeO at high pressure and temperature. Science. 1994;266(5191):1678–1680.

[65] Ozawa H, Hirose K, Ohta K, Ishii H, Hiraoka N, Ohishi Y, Seto Y. Spin crossover, structural change, and metallization in NiAs-type FeO at high pressure. Phys Rev B. 2011 Oct; 84:134417; Available from: http://link.aps.org/doi/10.1103/PhysRevB.84.134417.

[66] Hamada M, Kamada S, Ohtani E, Mitsui T, Masuda R, Sakamaki T, Suzuki N, Maeda F, Akasaka M. Magnetic and spin transitions in wüstite: A synchrotron Mössbauer spectroscopic study. Phys Rev B. 2016 Apr;93:155165; Available from: http://link.aps.org/doi/10.1103/PhysRevB.93.155165.

[67] Fischer RA, Campbell AJ, Lord OT, Shofner GA, Dera P, Prakapenka VB. Phase transition and metallization of FeO at high pressures and temperatures. Geophys Res Lett. 2011;38(24); l24301; Available from: http://dx.doi.org/10.1029/2011GL049800.

[68] Fischer RA, Campbell AJ, Shofner GA, Lord OT, Dera P, Prakapenka VB. Equation of state and phase diagram of feo. Earth and Plan Sci Lett. 2011;304(34):496 – 502; Available from: //www.sciencedirect.com/science/article/pii/S0012821X11000963.

[69] Ohta K, Cohen RE, Hirose K, Haule K, Shimizu K, Ohishi Y. Experimental and theoretical evidence for pressure-induced metallization in FeO with rocksalt-type structure. Phys Rev Lett. 2012 Jan;108:026403; Available from: http://link.aps.org/doi/10.1103/PhysRevLett.108.026403.

[70] Ohta K, Fujino K, Kuwayama Y, Kondo T, Shimizu K, Ohishi Y. Highly conductive iron-rich (Mg,Fe)O magnesiowstite and its stability in the Earth's lower mantle. J Geophys Res: Solid Earth. 2014;119(6):4656–4665; 2014JB010972; Available from: http://dx.doi.org/10.1002/2014JB010972.

[71] Knittle E, Jeanloz R, Mitchell AC, Nellis WJ. Metallization of $Fe_{0.94}O$ at elevated pressures and temperatures observed by shock-wave electrical resistivity measurements. Solid State

Commun. 1986 Aug;59:513–515.
[72] Speziale S, Milner A, Lee VE, Clark SM, Pasternak MP, Jeanloz R. Iron spin transition in Earth's mantle. Proc Natl Acad Sci USA. 2005;102(50):17918–17922; Available from: http://www.pnas.org/content/102/50/17918.abstract.
[73] Kantor I, Dubrovinsky L, McCammon C, Steinle-Neumann G, Kantor A, Skorodumova N, Pascarelli S, Aquilanti G. Short-range order and Fe clustering in $Mg_{1-x}Fe_xO$ under high pressure. Phys Rev B. 2009 Jul;80:014204; Available from: http://link.aps.org/doi/10.1103/PhysRevB.80.014204.
[74] Solomatova NV, Jackson JM, Sturhahn W, Wicks JK, Zhao J, Toellner TS, Kalkan B, Steinhardt WM. Equation of state and spin crossover of (Mg,Fe)O at high pressure, with implications for explaining topographic relief at the core-mantle boundary. Am Mineral. 2016; 101(5):1084–1093; Available from: http://ammin.geoscienceworld.org/content/101/5/1084.
[75] Isaak DG, Cohen RE, Mehl MJ, Singh DJ. Phase stability of wüstite at high pressure from first-principles linearized augmented plane-wave calculations. Phys Rev B. 1993 Apr; 47:7720–7731; Available from: http://link.aps.org/doi/10.1103/PhysRevB.47.7720.
[76] Badro J, Struzhkin VV, Shu J, Hemley RJ, Mao HK, Rueff JP, Kao CC. Iron partitioning in Earth's mantle: Toward a deep lower mantle discontinuity. Science. 2003;300:789–791.
[77] Lin JF, Struzhkin VV, Jacobsen SD, Hu M, Chow P, Kung J, Liu H, Mao HK, Hemley RJ. Spin transition of iron in magnesiowüstite in the Earth's lower mantle. Nature. 2005;436:377.
[78] Bagus PS, Brundle CR, Chuang TJ, Wandelt K. Width of the *d*-Level final-state structure observed in the photoemission spectra of Fe_xO. Phys Rev Lett. 1977 Nov;39:1229–1232; Available from: http://link.aps.org/doi/10.1103/PhysRevLett.39.1229.
[79] Fei Y, Zhang L, Corgne A, Watson H, Ricolleau A, Meng Y, Prakapenka V. Spin transition and equations of state of (Mg,Fe)O solid solutions. Geophys Res Lett. 2007;34(17); l17307; Available from: http://dx.doi.org/10.1029/2007GL030712.
[80] Tsuchiya T, Wentzcovitch RM, da Silva CRS, de Gironcoli S. Spin transition in magnesiowüstite in Earth's lower mantle. Phys Rev Lett. 2006 May;96:198501; Available from: http://link.aps.org/doi/10.1103/PhysRevLett.96.198501.
[81] Zhuravlev KK, Jackson JM, Wolf AS, Wicks JK, Yan J, Clark SM. Isothermal compression behavior of (Mg,Fe)O using neon as a pressure medium. Phys Chem Minerals. 2010; 37(7):465–474; Available from: http://dx.doi.org/10.1007/s00269-009-0347-6.
[82] Kuneš J, Křápek V. Disproportionation and metallization at low-spin to high-spin transition in multiorbital Mott systems. Phys Rev Lett. 2011 Jun;106:256401; Available from: http://link.aps.org/doi/10.1103/PhysRevLett.106.256401.
[83] Hu Q, Kim DY, Yang W, Yang L, Meng L Y Zhang, Mao HK. FeO_2 and FeOOH under deep lower-mantle conditions and Earth's oxygenhydrogen cycles. Nature. 2016 Jun;534:241–244.
[84] Otte K, Pentcheva R, Schmahl WW, Rustad JR. Pressure-induced structural and electronic transitions in FeOOH from first principles. Phys Rev B. 2009 Nov;80:205116; Available from: http://link.aps.org/doi/10.1103/PhysRevB.80.205116.
[85] Tunega D. Theoretical study of properties of goethite (α-FeOOH) at ambient and high-pressure conditions. The Journal of Physical Chemistry C. 2012;116(11):67036713; Available from: http://dx.doi.org/10.1021/jp2091297.
[86] Gleason A, Jeanloz R, Kunz M. Pressure-temperature stability studies of FeOOH using X-ray diffraction. Am Mineral. 2008;93(11-12):1882–1885; Available from: http://ammin.geoscienceworld.org/content/93/11-12/1882.